ChemComm

Accepted Manuscript

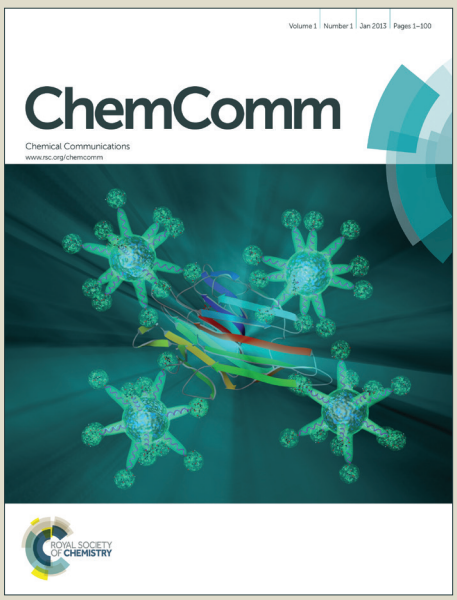

ROYAL SOCIETY OF CHEMISTRY

www.rsc.org/chemcomm

Journal Name

COMMUNICATION

Dual functionality of phosphonic acid appended phthalocyanines: inhibitors of urokinase plasminogen activator and anticancer photodynamic agents

Received 00th January 20xx,
Accepted 00th January 20xx

DOI: 10.1039/x0xx00000x

www.rsc.org/

N. Venkatramaiah,[a,b†] Patrícia M. R. Pereira,[a,c†] Filipe A. Almeida Paz,[b] Carlos A. F. Ribeiro,[c] Rosa Fernandes[c,d,e*] and João P. C. Tomé[a,f*]

Phthalocyanines (Pcs) bearing phosphonic acid groups at the periphery exhibits potential photodynamic efect to induce phototoxicity on human bladder cancer epithelial cells (UM-UC-3). The *in vitro* photophysical and biological studies show high intrensic ability to inhibit the activity of urokinase plasminogen activator (uPA) and matrix metalloproteinase-9 (MMP-9).

Considerable impetus has triggered in the design of novel amphiphilic photosensitizers (PSs) for photodynamic therapy (PDT), so to improve their water solubility and stability in generating reactive oxygen species (ROS).[1] Phthalocyanines (Pcs) are endowed with a certain degree of intrinsic properties as PSs due to their high ability to generate ROS, showing predominantly type-II photochemical reactions in the induction of cell death during PDT treatments.[2] The peripheral modification of Pcs with peptides, carbohydrates and protein functional units exhibit a new class of PSs with improved cancer cell target specificity, allowing very precise light induced cell destruction.[3-5] However, the core of Pcs has poor water solubility and consequently decrease in the production of ROS and phototoxicity.[6] Many derivatives were developed by covalent linking of Pcs with amphiphilic and ionic groups.[7-10] The presence of acid sensitive groups (–CO_2H and –SO_3H) at the periphery of Pcs and pH environment alter their stability, aggregation tendency and lipophilicity, which affect the cellular uptake process and photodynamic activity.[11,12] In this regard, the phosphonic acid groups are analogue to the carboxylic acid ones, having higher acidic strength. Compounds containing the former groups are described as inhibitors of serine proteases,[13] such as urokinase-type plasminogen activator (uPA).[14] The uPA is a valuable target in the development of new PSs for cancer PDT, because this enzyme plays a key role in cancer metastasis and cell invasion.[15] Similar to other serine proteases, uPA is secreted as catalytically latent pro-uPA, which is normally converted into active uPA by the action of proteases after it binds with receptor (uPAR). Activated uPA is involved on the degradation of the extracellular matrix (ECM) by converting the zymogen plasminogen into plasmin. The plasmin system is also involved on the activation of members of matrix metalloproteases (MMPs) able to promote degradation of the components of ECM.[16] Several strategies have been explored to target the uPA/uPAR system: (i) antisense oligonucleotides to interfere with the expression of these proteins; (ii) antibodies or competitive analogues to block the binding of uPA with uPAR; (iii) small molecule inhibitors to reduce the activity of uPA.[17,18] The inhibitory activity of PSs containing phosphonic acid against uPA has not been explored. We expect that the Pcs covalently linked to phosphonic acid moieties bear three important features: (i) Hydrophilic phosphonic acid head groups are sensitive to pH tuning, and can promote selectivity of Pcs towards cancer cells, since the pH in the tumors is lower than in normal tissues; (ii) Phosphonic acid compounds have an intrinsic ability to inhibit the uPA with high selectivity and potency during the tumor progression; (iii) Pcs can be activated in the near infrared region, which allows the delivery of light to within several centimeters of inaccessible tumors located deep under the body surface. As part of our continuing efforts in the development of efficient amphiphilic PSs for PDT,[19-21] herein, we describe the rational design and synthesis of novel Pcs bearing eight phosphonate type groups (protected and hydrolyzed) at peripheral positions. The photophysical/chemical properties, PDT effect and the inhibitory activity against uPA and matrix metalloproteinase-9 was investigated.

The synthetic route employed in the preparation of phosphonate functionalized Pcs was presented in Scheme 1. Tetraethyl(4,5-dicyano-1,2-phenylene)bisphosphonate(**P_2CN_2**) was obtained in 95% yield using a palladium-catalyzed cross-coupling reaction between 4,5-dichlorophthalonitrile and triethylphosphite under microwave irradiation at 230 °C for 45 min. Cyclotetramerization of **P_2CN_2** was failed with different metal ions in the presence of basic solvents such as DMAE, pyridine and quinoline with DBU at different temperatures. The optimized conditions were achieved by the addition of DBU at 80 °C in ethanol in a sealed glass tube under nitrogen

[a]*Department of Chemistry, QOPNA, University of Aveiro, 3810-193 Aveiro, Portugal. E-mail: jtome@ua.pt; Fax: +351 234370084; Tel: +351 234370342.*
[b]*Department of Chemistry, CICECO-Aveiro Institute of Materials, University of Aveiro, 3810-193 Aveiro, Portugal.*
[c]*Laboratory of Pharmacology and Experimental Therapeutics, Institute for Biomedical Imaging and Life Sciences (IBILI), Faculty of Medicine, University of Coimbra, 3000-548 Coimbra, Portugal. E-mail: rcfernandes@fmed.uc.pt; Fax: +351 239480066; Tel: +351 239480072.*
[d]*CNC.IBILI, University of Coimbra, Coimbra, Portugal.*
[e]*Center of Investigation in Environment, Genetics and Oncobiology, 3001-301 Coimbra, Portugal.*
[f]*Departmentof Organic and Macromolecular Chemistry, Ghent University, B-9000 Gent, Belgium.*
† These authors contributed equally to this work.
Electronic Supplementary Information (ESI) available: details of synthetic procedures, structural characterization (^{1}H, ^{31}P, ^{13}C NMR, MALDI-TOF MS, UV-Vis, steady-state and time-resolved fluorescence emission studies, details on the photochemical and biological assays. See DOI: 10.1039/c000000x/

atmosphere. When the temperature of the reaction was increased to 120 °C, shows the formation of desired green coloured octaphosphonate Pcs (**$H_2PcP_8E_{16}$** and **$ZnPcP_8E_{16}$**) in *ca.* 65% yields. The acid hydrolysis of these Pcs with 6 M HCl leads to de-cyclization of Pc into a monomeric hydrolyzed product identified as 1,3-dioxo-isoindoline-5,6-diyl)bis(phosphonic acid). Hence, the hydrolysis of the protected octaphosphonate Pcs was smoothly accomplished in 87% yield using trimethylsilyl bromide (TMSBr) in dry dichloromethane at room temperature.

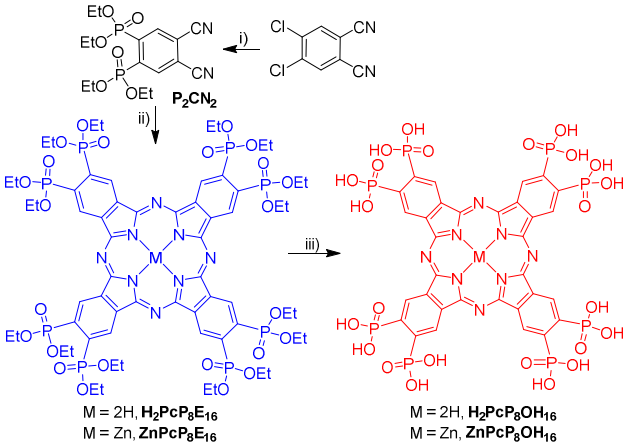

Scheme 1. i) P(OC2H5)3, Pd(PPh3)4, 230 ºC, 100 PSI, 120 W, 45 min; ii) Ethanol, DBU, 120 ºC, 12 h for H2PcP8E16 and ZnCl2, Ethanol, DBU, 120 ºC, 12 h for ZnPcP8E16; iii) TMSBr, dichloromethane, rt, 20 h.

The structure of the compounds was further corroborated using spectroscopic and spectrometric techniques (^{1}H, ^{13}C, ^{31}P NMR and MALDI-TOF and HR-MS; Figs. S1-S21, ESI†). The ^{1}H NMR spectra of **$H_2PcP_8E_{16}$** show the resonance of the NH protons at δ –3.24 ppm and α-protons of the isoindoline appears as a multiplet in the region δ 9.97–10.03 ppm, while the OCH_2 and CH_3 peaks are *ca.* δ 4.38 and δ 1.49 ppm, respectively (Fig. S5, ESI†). The vanishing of peaks in the aliphatic region and the presence of a triplet at δ 9.59 ppm (t, $^3J_{H\text{-}P}$ = 15 Hz) (due to long range coupling with the phosphorous nuclei) confirms the complete hydrolysis of the phosphoryl groups of **$H_2PcP_8E_{16}$**. ^{31}P NMR spectra of **$H_2PcP_8E_{16}$** and **$H_2PcP_8OH_{16}$** evidence multiplet and triplet peaks *ca.* δ 15.93-16.07 ppm and δ 12.7 ppm (t, $^3J_{H\text{-}P}$ = 15.7 Hz), while **$ZnPcP_8E_{16}$** and **$ZnPcP_8OH_{16}$** show a multiplet and triplet peaks at δ 14.93-15.07 ppm and δ 9.64 ppm (t, $^3J_{H\text{-}P}$ = 14.6 Hz). HR-MS spectra of all Pc derivatives exhibited molecular ion peaks at m/z 1603.40222 $[M+H]^+$, 1154.40320 $[M+H]^+$, 1665.29125 $[M+H]^+$ and 1216.90314 $[M+H]^+$ for **$H_2PcP_8E_{16}$**, **$H_2PcP_8OH_{16}$**, **$ZnPcP_8E_{16}$** and **$ZnPcP_8OH_{16}$**, respectively.

The phosphonate-appended Pcs exhibited, in water, Soret and Q-band absorption bands in the region *ca.* 335-395 nm and 605-710 nm, respectively. Free base Pcs show a split in the Q-band pattern while the Zn(II)Pcs show an intense Q-band (Fig. S22a, ESI†). The absorption behaviour of **$H_2PcP_8OH_{16}$** and **$ZnPcP_8OH_{16}$** demonstrated to be strongly dependent on the pH of the solution (Fig. S22b and Fig. S23-S25, ESI†). The absence of aggregation of Pcs containing phosphonic acid at pH ≥ 10 can be explained by full ionization of phosphonate groups, and, as a consequence, by a significant electrostatic repulsion of macrocycles carrying a large number of negative charges. In the pH ≈ 7-8, **$H_2PcP_8OH_{16}$** and **$ZnPcP_8OH_{16}$** retain the character of non-aggregate state. At pH < 5, a hypsochromic shift of Q band was observed. The intensity of the Q-band at *ca.* 696 nm decreases dramatically with the appearance of a weaker band at *ca.* 615 nm by changing the colour of the solution from green to blue. The appearance of a weaker absorption band *ca.* 615 nm is a characteristic of Pc aggregates[22] formed due to the phosphonic acid groups. At acidic pH, the phosphonic acid groups are partially ionized showing strong intermolecular hydrogen bonding interactions between phosphonate groups of other Pcs. This is expected to enhance aggregation by pulling individual Pc together. The emission spectra of the phosphonic acid derived Pcs, in water, are red-shifted by 14±2 nm when compared with the corresponding protected compounds, showing significant decrease in their emission intensities (Fig. S22c, ESI†). At acidic pH, the emission intensity of **$H_2PcP_8OH_{16}$** at 713 nm is quenched due to the formation of aggregates; its intensity increases significantly with increase in pH of the solution due to the formation of monomers (Fig. S22d, ESI†). Similar behaviour was observed for **$ZnPcP_8OH_{16}$**.

The fluorescence quantum yields (Table S1, ESI†) of Pcs were found to be in the range of 0.07−0.21 and follow the order **$ZnPcP_8E_{16}$** > **$H_2PcP_8E_{16}$** > **$ZnPcP_8OH_{16}$** > **$H_2PcP_8OH_{16}$**. The fluorescence lifetime of all phosphonate functionalized Pcs were found to be in the range of 4.12−4.68 ns (Fig. S26, ESI†). Table S1, ESI† summarizes the photophysical data of all phosphonate-functionalized Pc derivatives. The absorption and emission spectra of Pcs in DMF and in PBS (phosphate buffered saline) exhibited very similar absorption spectra with strong Q absorption bands at the red visible region (Fig. S27-S29, ESI†).

In DMF solution, the absorption spectra of Pcs in the Q-band region were broadened and increases linearly in intensity with respect to the concentration (2-50 μM) following the Beer-Lambert law. In PBS, the solubility of the Pcs increased in the order **$ZnPcP_8E_{16}$**≈**$H_2PcP_8E_{16}$**<**$ZnPcP_8OH_{16}$**≈**$H_2PcP_8OH_{16}$**. The Q-absorption bands of **$ZnPcP_8OH_{16}$**≈**$H_2PcP_8OH_{16}$** followed Beer-Lambert law for concentrations up to 30 μM, suggesting that water solubility was not compromised under these conditions.

The irradiation of the PBS solutions containing the Pc derivatives, with red light (620–750 nm) at a fluence rate of 50 $mW{\cdot}cm^{-2}$, resulted in a maximum of 12% decrease of the Q band intensity (Table S2, ESI†). These results clearly demonstrate that phosphonate Pc derivatives are almost photostable over a total irradiation period of 20 min. The photostability of phosphonate Pcs were higher than phosphonomethyl derivatives of metallophthalocyanines as reported.[23] The photosensitizing ability of the phosphonated Pcs to generate $^1O_2$ was determined using the steady-state method with DPBF as scavenger and **ZnPc** as reference. It was found that **$H_2PcP_8OH_{16}$** and **$ZnPcP_8OH_{16}$** have higher photosensitizing ability than protected phosphonate derivatives **$H_2PcP_8E_{16}$** and **$ZnPcP_8E_{16}$** (Fig. 1a). To screen the ability of Pc derivatives **$H_2PcP_8OH_{16}$** and **$ZnPcP_8OH_{16}$** to act as uPA inhibitors, a spectroscopic assay was performed using a chromogenic substrate, which is cleaved by active uPA enzyme.[24] The IC_{50} values, defined as the concentration of Pc able to inhibit 50% of uPA activity were obtained from the data collected in Fig. 1b. **$H_2PcP_8E_{16}$** and **$ZnPcP_8E_{16}$** were not able to inhibit uPA. **$H_2PcP_8OH_{16}$** and **$ZnPcP_8OH_{16}$** inhibited uPA with IC_{50} values of 1.154 and 1.476 μM, respectively. These results combined with the high ability of these Pc derivatives to generate $^1O_2$ after light irradiation motivated us to determine their photo-cytotoxicity against human bladder cancer cells as well as their ability to inhibit uPA enzyme directly in these cells. The *in vitro* photodynamic properties of phosphonate appended Pcs were determined using the human bladder cancer

epithelial cell line UM-UC-3. Additional studies were also performed in a non-tumoral epithelial cell line (ARPE-19).

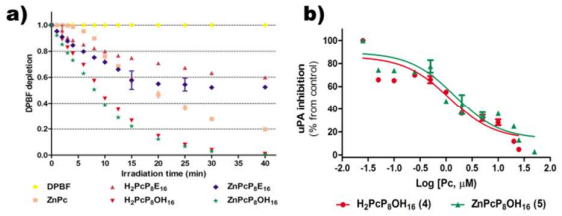

Fig. 1. (**a**) Photo-oxidation of DPBF (25 μM) in DMF:H_2O (9:1) with or without **$H_2PcP_8E_{16}$**, **$H_2PcP_8OH_{16}$**, **$ZnPcP_8E_{16}$**, **$ZnPcP_8OH_{16}$** or **ZnPc** at 0.25 μM, after irradiation with a LED array system emitting red light at a fluence rate of 10 mW·cm^{-2}. The DPBF absorbance was recorded at 415 nm. (**b**) Dose response curves of uPA activity to **$H_2PcP_8OH_{16}$** and **$ZnPcP_8OH_{16}$**. Data are the mean value ± S.D. of at least two independent experiments. The lines represent the fit to a sigmoid model.

As shown in Fig. S30, ESI† and Fig. 2a, compounds **$H_2PcP_8OH_{16}$** and **$ZnPcP_8OH_{16}$** demonstrated higher ability to be accumulated inside the bladder cancer cells when compared with their protected counterparts. Additionally, the uptake of **$H_2PcP_8OH_{16}$** and **$ZnPcP_8OH_{16}$** was higher in UM-UC-3 cancer cells than in ARPE-19 cells. The spectrofluorimetric data was confirmed by confocal microscopy showing that incubation of cancer cells with Pcs at 2 μM for 2 h in darkness led to the uptake of all compounds resulting in intracellular fluorescence (Fig. 2b).

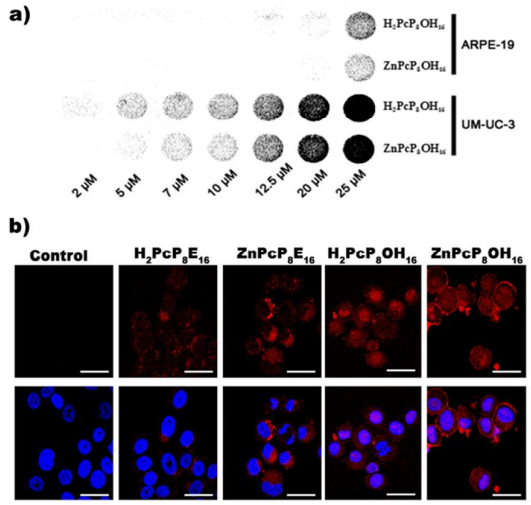

Fig. 2. (**a**) Spectroscopic images of UM-UC-3 and ARPE-19 cells incubated with Pcs. (**b**) Fluorescence microscopic images of UM-UC-3 bladder cancer cells incubated with Pcs (red) in darkness and the cell nucleus stained with DAPI (blue). *Scale bars 20 μm*.

The accumulation of phosphonic acid Pc derivatives in cancer cells can be explained by a non-specific mechanism caused by reduction of the membrane permeability barrier towards amphiphilic Pcs. Knowing that tumors have low pH in the extracellular region when compared with that around normal tissues,[25] we expect that the acidic environment of the cancer cells affect the protonation of the phosphonic acid groups in **$H_2PcP_8OH_{16}$** and **$ZnPcP_8OH_{16}$**, thus significantly increasing its capacity to freely cross the plasma membrane. Having established that the new compounds inhibit uPA (Fig. 1b) and accumulate in cancer cells (Fig. 2), we analyzed the effect of Pcs in the activity of cancer cell surface-bound uPA and further evaluated the impact on MMP-9 activity and protein expression. Fluorometric assays were conducted using the fluorogenic uPA-selective substrate Glutaryl-Gly-Arg Amino Methyl Cumarin (AMC) in the conditioned medium of UM-UC-3 cancer cells. In this assay, active uPA digests the synthetic substrate releasing the fluorescent free AMC. The positive controls Glu-Gly-Arg-chloromethyl ketone (commercial uPA inhibitor) and uPA standard were included for assay validation. The commercial uPA inhibitor showed potent inhibition of cell-bound uPA (Fig. S31, ESI†). Compounds **$H_2PcP_8E_{16}$** and **$ZnPcP_8E_{16}$** at 2 μM produced no reduction of fluorescence relative to control (cells in the absence of compounds) indicating that they do not reduce the activity of uPA in cancer cells. The same concentration of **$H_2PcP_8OH_{16}$** and **$ZnPcP_8OH_{16}$** reduced the observed fluorescence relative to control cells by 44.74% and 55.93%, respectively.

The conversion of the zymogen plasminogen into the active plasmin by uPA is a key event during the invasion of bladder cancer through the ECM. In this process, plasmin activates the pericellular proteolysis of ECM components and activates MMPs.[26,27] MMP-9 promotes bladder cancer associated proteolysis, being important for cancer progression.[28] Therefore, we determined whether the inhibition of uPA by the new compounds can induce effects on the activity of MMP-9 in UM-UC-3 cancer cells. Gelatin zymography was performed using the conditioned medium of UM-UC-3 cancer cells. As shown in Fig. 3a, **$H_2PcP_8OH_{16}$** and **$ZnPcP_8OH_{16}$** significantly reduced the gelatinolytic activity of MMP-9 from cancer cells. Consistent with the inhibition of gelatinolytic activity, Western blot analysis of the conditioned medium also revealed that **$H_2PcP_8OH_{16}$** and **$ZnPcP_8OH_{16}$** down regulated the level of active form of MMP-9 (82 kDa) (Fig. 3b). These results indicated that the ability of **$H_2PcP_8OH_{16}$** and **$ZnPcP_8OH_{16}$** to inhibit uPA also results on the inhibition of MMP-9.

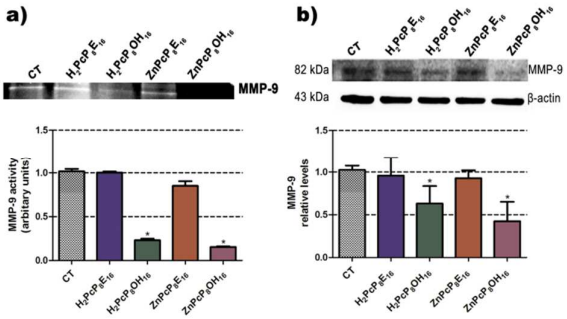

Fig. 3. (**a**) Gelatin zymography and quantitative analysis of uPA activity expressed as a ratio of the activity found in conditioned medium of control UM-UC-3 cancer cells. (**b**) Western blotting analysis and quantification of MMP-9 protein levels in conditioned medium of UM-UC-3 cancer cells. β-actin was blotted as loading control. Data are mean ± S.D. of three independent experiments.*($p<0.05$), ***($p<0.0001$) significantly different from control cells.

After assessment of the Pcs uptake, their toxic potential in the presence and absence of light was evaluated in both UM-UC-3 cancer cells and ARPE-19 cells. No dark toxicity was observed in both cell lines incubated with the Pcs (up to 25 μM) for 2 h (Figs. S32 and S33, ESI†). The PDT assays were then performed in cells previously incubated for 2 h with different concentrations of Pcs (0.025-25 μM) and irradiated with red light (620-750 nm) at 4.5 mW·cm^{-2} during 20 min. None of the compounds induced significant phototoxicity in ARPE-19 cells (Fig. S33, ESI†). In UM-UC-3 cancer cells, data showed interesting differences between the compounds containing

phosphonate groups and those bearing phosphonic acid groups. The latter were able to induce phototoxicity in a concentration dependent manner, which was higher when compared with that of $\mathbf{H_2PcP_8E_{16}}$ and $\mathbf{ZnPcP_8E_{16}}$ (Fig. S34, ESI†). The concentration of Pcs that inhibits the metabolic activity of UM-UC-3 bladder cancer cells in 50% (IC_{50}) was estimated from the data summarized in Fig. 4a. These IC_{50} values, were similar for $\mathbf{H_2PcP_8OH_{16}}$ (2.068 μM) when compared with $\mathbf{ZnPcP_8OH_{16}}$ (2.272 μM). These values were similar to that derived for galactodendritic conjugated Pc against UM-UC-3 bladder cancer cells.[21]

Knowing that ROS have a critical role in the induction of cell death after PDT and considering the different PDT induced phototoxicity observed with these Pc derivatives in UM-UC-3 bladder cancer cells, the intracellular production of ROS was evaluated immediately after PDT. The PDT with $\mathbf{H_2PcP_8OH_{16}}$ and $\mathbf{ZnPcP_8OH_{16}}$ led to higher ROS production when compared with that of the protected forms (Fig. 4b). To determine the contribution of cytotoxic ROS generated after PDT with $\mathbf{H_2PcP_8OH_{16}}$ and $\mathbf{ZnPcP_8OH_{16}}$, quenchers of ROS (sodium azide, histidine and cysteine) were added at non-toxic concentrations to the incubation medium when the cells were irradiated (Fig. S35, ESI†). Data show that $^1O_2$ should have a high effect in the phototoxicity induced by $\mathbf{H_2PcP_8OH_{16}}$ and $\mathbf{ZnPcP_8OH_{16}}$ because the inhibition of metabolic activity was highly reduced with sodium azide (*i.e.* a quencher of $^1O_2$).[29,30]

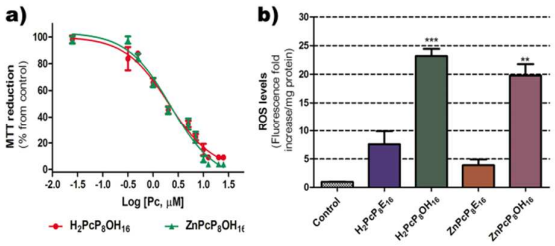

Fig. 4. (**a**) Dose response curves of UM-UC-3 cancer cells to $\mathbf{H_2PcP_8OH_{16}}$ and $\mathbf{ZnPcP_8OH_{16}}$. Data are the mean value ± S.D. of at least three independent experiments performed in triplicates. The lines represent the fit to a sigmoid model. (**b**) Quantification of DCF fluorescence increase (as a measure of ROS production) in UM-UC-3 cells, after PDT with $\mathbf{H_2PcP_8OH_{16}}$ or $\mathbf{ZnPcP_8OH_{16}}$. Data are the mean ± S.D. of at least three independent experiments performed in triplicates. **(p<0.001), ***(p<0.0001) significantly different from control cells.

In summary, novel Pc derivatives covalently appended with phosphonate groups at periphery was prepared and evaluated as anticancer agents.The Pcs containing phosphonic acid groups, $\mathbf{ZnPcP_8OH_{16}}$ and $\mathbf{H_2PcP_8OH_{16}}$, exhibit strong pH-dependent photophysical properties and demonstrated high ability to produce $^1O_2$ and to inhibit the activities of uPA and MMP-9. The presence of phosphonic acid groups on Pcs quench the fluorescence behaviour and show enhanced ability to generate $^1O_2$ and furnish potent and specific PDT effect against human bladder cancer cells. $\mathbf{ZnPcP_8OH_{16}}$ and $\mathbf{H_2PcP_8OH_{16}}$ exhibited higher accumulation inside bladder cancer cells, higher intracellular ROS generation (namely $^1O_2$) than the corresponding $\mathbf{ZnPcP_8E_{16}}$ and $\mathbf{H_2PcP_8E_{16}}$, with consequently higher phototoxicity. Tuning the structural modification of Pcs with different phosphonic acid groups provides useful strategy to enhance the efficacy of this class of therapeutic agents. Further advances towards to understand the pH-dependent photophysical and photobiological behaviour of $\mathbf{ZnPcP_8OH_{16}}$ and $\mathbf{H_2PcP_8OH_{16}}$ and their direct impact (before and after PDT) on the activity of uPA in UM-UC-3 bladder cancer cells are under investigation.

Notes and references

Thanks are due to FCT/MEC for the financial support to QOPNA research Unit (FCT UID/QUI/00062/2013), IBILI research Unit (FCT UID/NEU/04539/2013) and CICECO-Aveiro Institute of Materials (FCT UID/CTM/50011/2013), through national founds and where applicable co-financed by the FEDER, within the PT2020 Partnership Agreement, and also to the Portuguese NMR Network. We further wish to thank FCT for funding the R&D project (EXPL/CTM-NAN/0013/2013; FCOMP-01-0124-FEDER-041282). The authors also acknowledge FCT for the post-doctoral and doctoral research grants SFRH/BPD/79000/2011 (to NVR) and SFRH/BD/85941/2012 (to PMRP), respectively.

1. M. Ethirajan, Y. Chen, P. Joshi and R. K. Pandey, *Chem. Soc. Rev*., 2011, **40**, 340.
2. R. Bannet, *Chem. Soc. Rev*., 1995, **24**, 19.
3. E. Ranyuk , N. Cauchon , K. Klarskov, B. Guérin, and J. E. Lier, *J. Med. Chem.*, 2013, **56**, 1520.
4. A. R. Soares, J. P. C. Tomé, M.G.P.M.S. Neves, A. C. Tomé, J. A. Cavaleiro and T. Torres, *Carbohydr. Res*., 2009, **344**, 507.
5. A. Ogunsipea and T. Nyokong, *Photochem.Photobiol. Sci*., 2005, **4**, 510.
6. V. V. Koval, A. A. Chernonosov, T. V. Abramova, T. M. Ivanova, O. S. Federova, V. M. Derkacheva and E. A. Lukyantes, *Nucleosides, Nucleotides Nucleic Acids*, 2001, **4**, 1259.
7. F. Dumoulin, M. Durmuş,V. Ahsen and T. Nyokong, *Coord. Chem. Rev*., 2010, **254**, 2792.
8. J. B. Pereira, E. F. A. Carvalho, M. A. F. Faustino, R. Fernandes, M. G. P. M. S. Neves, J. A. S. Cavaleiro, N. Gomes, Â. Cunha, A. Almeida, J. P. C. Tomé, *Photochem. Photobiol*, 2012, **88**, 537.
9. L. M. O. Lourenço, M. G. P. M. S. Neves, J. A. S. Cavaleiro, J. P. C. Tomé, *Tetrahedron* 2014, **70**, 268.
10. D. Çakır, M. Göksel, V. Çakır, M. Durmuş, Z. Biyiklioglu and H. Kantekin, *Dalton Trans*., 2015, **44**, 9646.
11. X. J. Jiang, P. C. Lo, S. L. Yeung, W. P. Fong and D. K. P. Ng, *Chem. Commun*., 2010, **46**, 3188.
12. M. R. Ke, D. K. P. Ng and P. C. Lo, *Chem. Commun*., 2012, **48**, 9065.
13. H. R. Almond, S. Cesco-Cancian, G. L. De, M. N. Greco, M. J. Hawkins, M. J. Humora, B. E. Maryanoff, C. N. Nilsen, M. N. Patel and Y. Qian, US Patent, US 8,394,804 B2, 2013.
14. S. Rosenberg, *Annu. Rep. Med. Chem*., 1999, **34**, 121.
15. M. J. Duffy, *Clin Cancer Res*, 1996, **2**, 613.
16. A. F. Chambers and L. M. Matrisian, *J. Natl. Cancer Inst*. 1997, **89**, 1260.
17. M. Schmitt, O. G. Wilhelm, U. Reuning, A. Krüger, N. Harbeck, E. Lengyel, H. Graeff, B. Gänsbacher, H. Kessler, M. Bürgle, J. Stürzebecher, S. Sperl, V. Magdolen, *Fibrinol. Proteol*.2000, **14** 114.
18. T. W. Rockway, V. Nienaber and V. L. Giranda, *Curr. Pharm. Des*., 2002, **8**, 2541.
19. S. Silva, P. M. R. Pereira, P. Silva, F. A. Almeida Paz, M. A. F. Faustino, J. A. S. Cavaleiro and J. P. C. Tomé ,*Chem. Commun.*, 2012, **48**, 3608.
20. L. M. O. Lourenço, P. M. R. Pereira, E. Maciel, M. Válega, F. M. J. Domingues, M.R. M. Domingues, M. G. P. M. S. Neves, J. A. S. Cavaleiro, R. Fernandes and J. P. C. Tomé ,*Chem. Commun.*, 2014, **50**, 8363.
21. P. M. R. Pereira, S. Silva, J. A. S. Cavaleiro, C. A. F. Ribeiro, J. P. C. Tomé and R. Fernandes, *Plos One*, 2014, **9**, e95529.
22. N. Venkatramaiah, D. M. G. C. Rocha, P. Srikanth, F. A. A. Paz, J. P. C. Tomé, *J. Mater. Chem. C*, 2015, **3**, 1056.
23. A. N. Komissarov, D. A. Makarov, O. A. Yuzhakova, L. P. Savvina, N. A. Kuznetsova, O. L. Kaliya, E. A. Lukyanets and V. M. Negrimovsky, *Macroheterocycles,*. 2012, **5**, 169.
24. M. A. AlShaer, M. A. Khanfar and M. O. Taha, *J. Mol. Model*, 2014, 20.
25. J. Moan, L. Smedshammer, T. Christensen, *Cancer Lett.*, 1980, **9**, 27.
26. M.J. Duffy, *Curr Pharm Des*., 2004, **10**, 39.
27. F. J. Castellino, Plopplis V A, *Trromb Haemost*, 2005, **93**, 647.
28. K.Vasala, P. Pääkko, T. Turpeenniemi-Hujanen, *Anticaner Res,* 2008, **28**, 1757.
29. M. Bancirova, *Luminescence*, 2011, **26**, 685.
30. O. I. Aruoma, B. Halliwell, B. M. Hoey and J. Butler, *Free Radical Bio Med*, 1989, **6**, 593.